ORGANIC LETTERS

2012
Vol. 14, No. 11
2698–2701

Zinc(II) Mediated Imine–Enamine Tautomerization

Prem N. Basa, Arundhati Bhowmick, LaShawn Medicine Horn, and Andrew G. Sykes*

Department of Chemistry, University of South Dakota, Vermillion, South Dakota 57069, United States

asykes@usd.edu

Received April 5, 2012

ABSTRACT

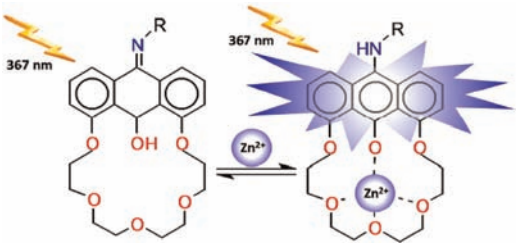

Reduction of imine–anthracenone compounds selectively produces secondary alcohols leaving the external imine group unreacted. Addition of the Zn(II) ion induces a metal-mediated imine–enamine tautomerization reaction that is selective for Zn(II), a new fluorescence detection method not previously observed for this important cation.

Elevated levels of zinc are known to play a key role in potential neurological disorders such as Alzheimer's and Parkinson's disease;[1] however a detailed understanding of the role played by the Zn(II) ion in cell homeostasis, signal transduction, and translocation still remains a challenge. Within the past decade, pioneering research in PET,[2] ICT,[3] FRET,[4] and other[5] based fluorescent chemosensors have made significant progress in understanding the bioinorganic chemistry and coordination properties of Zn(II), and recent advances in C=N isomerization of imine-containing fluorescence sensors selective for Zn(II) have also proven to be an attractive tool.[6]

Imines are typically more stable than their enamine tautomers;[7] however, the energy barrier for imine–enamine interconversion is an order of magnitude smaller than that for the isoelectronic keto–enol tautomerization,[8] which allows preparative/catalytic procedures to be developed involving enamine intermediates.[9] We have recently reported the site-selective imination of anthraquinone-containing macrocycles (analogues similar to **2a**–**b** in Scheme 1) and have explored the host/guest chemistry of these new adducts as fluorescence sensors.[10] Herein we report the selective reduction of the internal carbonyl group (**3a**–**b**) and the resulting 1,5-prototopic shift involving metal-mediated

(1) (a) Xu, Z.; Yoon, J.; Spring, D. R. *Chem. Soc. Rev.* **2010**, *39*, 1996. (b) Que, E. L.; Domaille, D. W.; Chang, C. J. *Chem. Rev.* **2008**, *108*, 1517.

(2) (a) Xu, Z.; Baek, K.-H.; Kim, H. N.; Cui, J.; Qian, X.; Spring, D. R.; Shin, I.; Yoon, J. *J. Am. Chem. Soc.* **2009**, *132*, 601. (b) Burdette, S. C.; Lippard, S. J. *Inorg. Chem.* **2002**, *41*, 6816. (c) Zhang, X.-a.; Hayes, D.; Smith, S. J.; Friedle, S.; Lippard, S. J. *J. Am. Chem. Soc.* **2008**, *130*, 15788. (d) Nolan, E. M.; Ryu, J. W.; Jaworski, J.; Feazell, R. P.; Sheng, M.; Lippard, S. J. *J. Am. Chem. Soc.* **2006**, *128*, 15517.

(3) (a) Maruyama, S.; Kikuchi, K.; Hirano, T.; Urano, Y.; Nagano, T. *J. Am. Chem. Soc.* **2002**, *124*, 10650. (b) Komatsu, K.; Urano, Y.; Kojima, H.; Nagano, T. *J. Am. Chem. Soc.* **2007**, *129*, 13447. (c) Lu, C.; Xu, Z.; Cui, J.; Zhang, R.; Qian, X. *J. Org. Chem.* **2007**, *72*, 3554. (d) Zhang, Y.; Guo, X.; Si, W.; Jia, L.; Qian, X. *Org. Lett.* **2008**, *10*, 473.

(4) (a) Sreenath, K.; Allen, J. R.; Davidson, M. W.; Zhu, L. *Chem. Commun.* **2011**, *47*, 11730. (b) Vinkenborg, J. L.; Nicolson, T. J.; Bellomo, E. A.; Koay, M. S.; Rutter, G. A.; Merkx, M. *Nat. Meth.* **2009**, *6*, 737.

(5) (a) Du, P.; Lippard, S. J. *Inorg. Chem.* **2010**, *49*, 10753. (b) Tamanini, E.; Katewa, A.; Sedger, L. M.; Todd, M. H.; Watkinson, M. *Inorg. Chem.* **2008**, *48*, 319. (c) Hanaoka, K.; Kikuchi, K.; Kojima, H.; Urano, Y.; Nagano, T. *J. Am. Chem. Soc.* **2004**, *126*, 12470. (d) Zhou, X.; Yu, B.; Guo, Y.; Tang, X.; Zhang, H.; Liu, W. *Inorg. Chem.* **2010**, *49*, 4002. (e) Lim, N. C.; Schuster, J. V.; Porto, M. C.; Tanudra, M. A.; Yao, L.; Freake, H. C.; Brückner, C. *Inorg. Chem.* **2005**, *44*, 2018. (f) Li, Y.; Shi, L.; Qin, L.-X.; Qu, L.-L.; Jing, C.; Lan, M.; James, T. D.; Long, Y.-T. *Chem. Commun.* **2011**, *47*, 4361. (g) Sun, F.; Zhang, G.; Zhang, D.; Xue, L.; Jiang, H. *Org. Lett.* **2011**, *13*, 6378.

(6) (a) Wu, J.; Liu, W.; Ge, J.; Zhang, H.; Wang, P. *Chem. Soc. Rev.* **2011**, 40. (b) Jung, H. S.; Ko, K. C.; Lee, J. H.; Kim, S. H.; Bhuniya, S.; Lee, J. Y.; Kim, Y.; Kim, S. J.; Kim, J. S. *Inorg. Chem.* **2010**, *49*, 8552.

(7) Lin, J.-F.; Wu, C.-C.; Lien, M.-H. *J. Phys. Chem.* **1995**, *99*, 16903.

(8) Lammertsma, K.; Prasad, B. V. *J. Am. Chem. Soc.* **1994**, *116*, 642.

(9) Notz, W.; Tanaka, F.; Barbas, C. F. *Acc. Chem. Res.* **2004**, *37*, 580.

(10) Basa, P. N.; Bhowmick, A.; Schulz, M. M.; Sykes, A. G. *J. Org. Chem.* **2011**, *76*, 7866.

10.1021/ol300874c
Published on Web 05/14/2012

imine-enamine tautomerization resulting in enhancement in anthracene emission, selective for the Zn(II) ion (Scheme 1).

Compounds **2a**–**b** have been synthesized and characterized by our previously reported procedure.[10] Here the carbonyl group has been selectively reduced to the corresponding 2° alcohols, **3a**–**b**, using sodium borohydride in ethanol (Scheme 1), leaving the imine functionality intact.

Scheme 1. Synthesis and Reactivity of Imine–Anthracenone Compounds

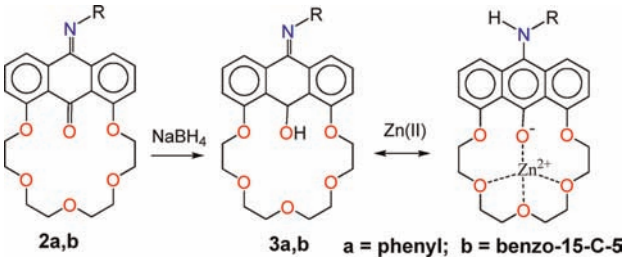

The reduction of the carbonyl group is confirmed by FT-IR, ^{1}H NMR, and ^{13}C NMR spectroscopic data (Figures S1–S14, Supporting Information). FT-IR analysis of compounds **3a**–**b** shows a new broad peak at 3400–3500 cm^{-1} which is characteristic of the –OH group that is not seen in the unreduced compounds, **2a**–**b**. In addition, the strong resonance for the internal carbonyl C=O stretch (~1670 cm^{-1}) disappears after reduction; however an imine stretching frequency (1660–1675 cm^{-1}) still remains. ^{13}C NMR spectra reveal a new peak at (~57 ppm) for the reduced CH(OH) carbon, and the peak for the carbonyl carbon (~180 ppm) disappears. The peak for the C=N carbon (~158.4 ppm) remains upon reduction however. Such spectroscopic data indicate that only the carbonyl group (C=O) has been selectively reduced. In addition, ESI-MS spectra of compounds **3a**–**b** show MH^+ and MNa^+ peaks consistent with a single reduction (Figures S7 and S11).

Structural confirmation by X-ray crystallography of compound **3a** has also been determined (Figure 1). The hydroxyl group O(1) is bound to an sp^3 hybridized carbon, while the imine carbon remains sp^2 hybridized and exhibits C(10)–N(2) = 1.285(3) Å, an interatomic distance typical of C=N double bonds. The hydroxyl proton was also observed from the difference map and is involved in a hydrogen bond with the nitrogen atom of the neighboring acetonitrile molecule.

Addition of Zn(II) to compounds **3a**–**b** all show the growth of new fluorescence peaks characteristic of an anthracene emission manifold (Figures 2, 4 and Supporting Information) We propose that these new reduced compounds undergo imine–enamine tautomerization to form the fully conjugated, three-ring anthracene π-system (Scheme 1). Imine–enamine tautomerization may also explain why reduction of the imine does not take place as usual with $NaBH_4$. Reduction of the more electronegative

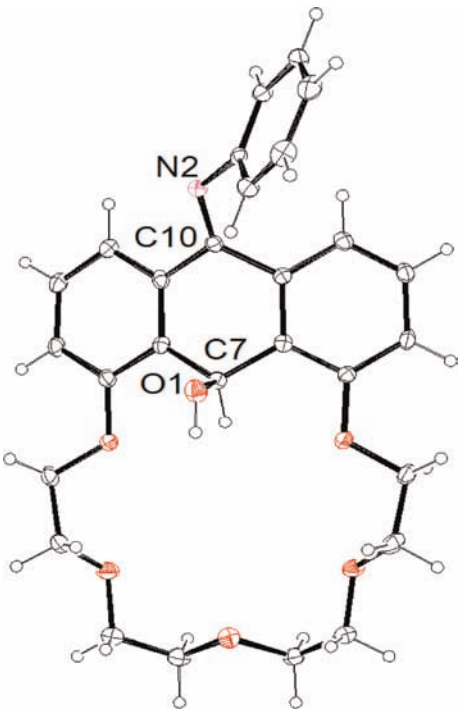

Figure 1. X-ray crystal structure (30%) of **3a**·CH_3CN. C(10)–N(2) = 1.285(3) Å, C(7)–O(1) = 1.439(3) Å, and C(10)–N(2)–C(15) = 121.6(2)°. One intermolecular hydrogen bond exists in the structure between the hydroxyl proton and a neighboring acetonitrile: O(1)–H(99)···N(1) = 2.835(4) Å. The acetonitrile solvent molecule has been removed from the thermal ellipsoid diagram for clarity.

carbonyl group occurs first, followed by imine–enamine tautomerization preventing further imine reduction. Compound **4**[11] (the anthraquinone analogue without the imine group) does not produce growth in anthracene fluorescence with added Zn(II) ion, since keto–enol tautomerization has a higher conversion barrier (Scheme S1). In addition, the fluorescence properties of the fully reduced anthracene analogue, compound **5**,[12] was compared and the emission manifold is almost identical to that of compounds **3a**–**b** plus added Zn(II) (Figure S15).

Titration of a 50:50 acetonitrile/water mixture of **3a** with Zn(II) produces a 1:1 ligand–metal formation as evidenced by the saturation in the fluorescence data at 1.0 equiv of added zinc (Figure 2 and insert). Fitting the data to an L + Zn(II) → LZn(II) stoichiometry (solid line) results in a binding constant of ~1.0×10^5 (±10%) M^{-1}. Additional evidence for 1:1 Zn(II) complex formation comes from the ESI-MS data. Upon addition of 3.0 equiv of the Zn(II) to **3b** in acetonitrile, a new peak at 729 m/z appears, which corresponds to the MZn^+ parent ion as shown in Figure S16. The 729 *m*/*z* MZn^+ parent ion dominates when 10.0 equiv of Zn(II) are added (Figure S17). The hydroxyl proton is deprotonated in this case, and the anion

(11) Kadarkaraisamy, M.; Caple, G.; Gorden, A. R.; Squire, M. A.; Sykes, A. G. *Inorg. Chem.* **2008**, *47*, 11644.

(12) (a) Lu, L.; Chen, Q.; Zhu, X.; Chen, C. *Synthesis* **2003**, *2003*, 2464. (b) Hua Jiang, H. X.; Xia, P.; Zhou, Q. *Chin. Chem. Lett.* **1999**, *10*, 1015.

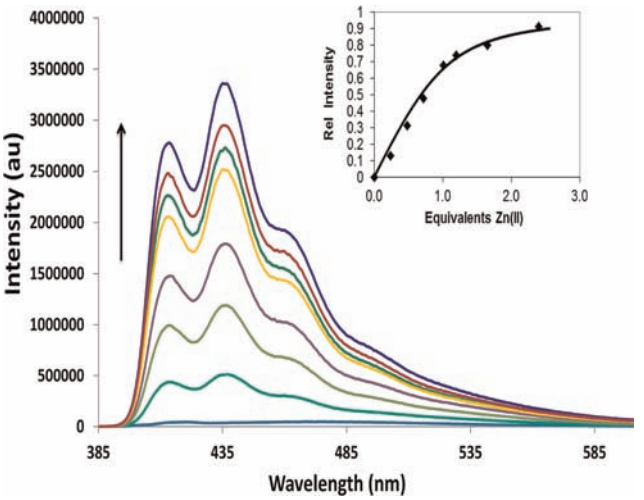

Figure 2. Fluorescence titration of 5.0×10^{-5} M of compound **3a** in acetonitrile/water (50:50) mixture with increasing amounts of Zn(II), $\lambda_{ext} = 367$ nm. Inset, intensity vs equiv of Zn(II), monitored at 434 nm.

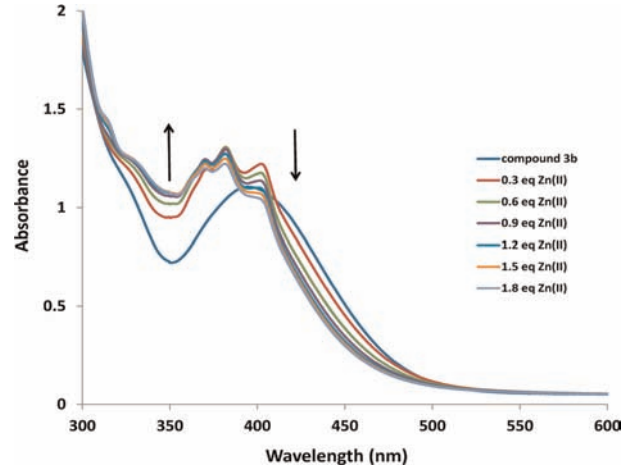

Figure 3. UV−vis spectrum of compound **3b** (4.0×10^{-5} M), upon increasing addition of the Zn(II) in acetonitrile.

formed is stabilized by the Zn(II) trapped within the polyether ring. The single negative charge of the host and the double positive charge of the Zn(II) ion form the MZn^+ singly charged parent ion (Scheme 1). In addition, the MS/MS spectrum of the 729 *m*/*z* parent ion peak was obtained (Figure S18) which shows a main 462 *m*/*z* fragment ion which corresponds exactly to the loss of the benzo-15-crown-5 ring, necessitating that the Zn cation be located in the larger polyether ring containing the intraannular oxygen. ^{1}H NMR titrations of compound **3b** with increasing addition of Zn(II) in CD_3CN also show a loss of the anthrone hydroxyl proton and anthrone C−H proton at 5.7 and 6.8 ppm (Figure S19).

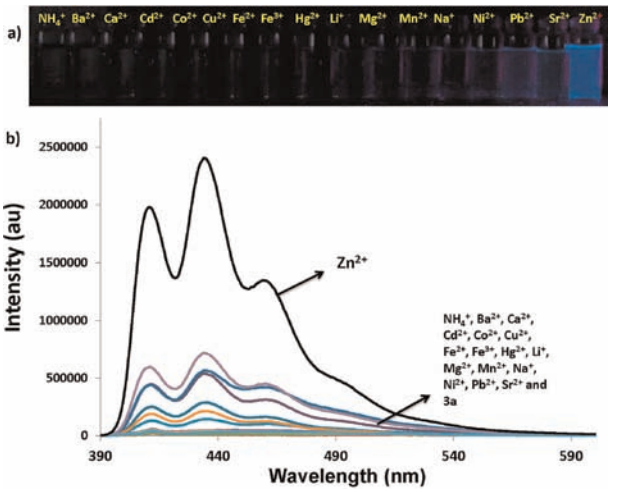

Figure 4. (a) Photograph and (b) fluorescence emission spectra of compound **3a** (4.0×10^{-5} M) verses 1.2×10^{-2} M, 5.0 equiv of metal salts, NH_4^+, Ba^{2+}, Ca^{2+}, Cd^{2+}, Co^{2+}, Fe^{2+}, Fe^{3+}, Hg^{2+}, Li^+, Mg^{2+}, Mn^{2+}, Na^+, Ni^{2+}, Pb^{2+}, Sr^{2+}, Zn^{2+}, and Cu^{2+} in acetonitrile at $\lambda_{ext} = 367$ nm.

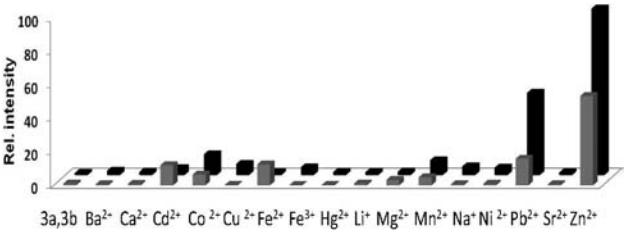

Figure 5. A 3D bar graph showing fluorescence enhancement of compound **3a** (front, gray) and **3b** (back, black),with respect to metal ions, monitored at 430 nm. $\lambda_{ext} = 367$ nm was used for compounds **3a**−**b**.

The UV-vis titration of compound **3b** with Zn(II) produces the characteristic absorbance manifold for anthracene, essentially the mirror image of the emission manifold (Figure 3). Also polar protic solvents show slight blue shifts in emission and absorption maxima as compared to nonpolar aprotic solvents (Figures S20−S21).

UV−vis and fluorescence responses were observed for compounds **3a**−**b** with the addition of 5.0 equiv of perchlorate salts of NH_4^+, Ba^{2+}, Ca^{2+}, Cd^{2+}, Co^{2+}, Cu^{2+}, Fe^{2+}, Fe^{3+}, Hg^{2+}, Li^+, Mg^{2+}, Mn^{2+}, Na^+, Ni^{2+}, Pb^{2+}, Sr^{2+}, Zn^2 in acetonitrile, and the resulting spectra were recorded after 4 min (Figures 4, 5 and S20−S22). Compounds **3a** and **3b** have similar selectivity for Zn(II); however compound **3b** shows the greatest fluorescence enhancement for the Zn(II) ion (~100-fold) as compared to **3a** (~50-fold). Pb(II) is the only other cation that showed spectral interference, where the same high affinity for Pb(II) has previously been observed

(13) Kadarkaraisamy, M.; Sykes, A. G. *Inorg. Chem.* **2005**, *45*, 779.

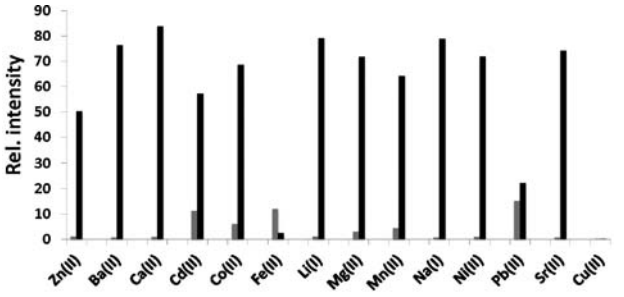

Figure 6. Selectivity−Competition study of compound **3a** with added M(II) perchlorate salts (5.0 equiv) followed by 1.0 equiv of added Zn(II). 4.0×10^{-5} M = [**3a**], λ_{ext} = 367 nm. Fluorescence intensity monitored at 434 nm: Gray = **3a** + 5.0 equiv of M(II); Black = **3a** + 5.0 equiv of M(II) + 1.0 equiv of Zn(II).

for the parent anthraquinone macrocycle.[13] Interference from Cd(II) and Hg(II), members of the same family, is not observed in this case which is common with many other fluorescence detection systems for Zn(II).

A competition experiment was carried out for compound **3a** (Figures 6, S25), showing good selectivity for Zn(II) in the presence of most other cations. Pb(II) remains competitive for the binding site, and the paramagnetic cations Fe(II) /Cu(II) quench the emission. The influence of pH on Zn(II) induced fluorescence was investigated by taking a 1:1 mixture (acetonitrile/water) of compound **3b** (4.0×10^{-5} M) and buffered solutions of pH 1.0−10.0. The intensity remained unaffected at the pH range 6.0−8.0, thus suggesting that the sensor is suitable for physiological applications (Figure S26).

In summary, we have selectively reduced the internal carbonyl of new imine compounds with $NaBH_4$, leaving the external imine intact as confirmed by FTIR, ^{1}H NMR, ^{13}C NMR, ESI-MS, elemental analyses and single-crystal X-ray crystallography. The fluorescence emission pattern upon addition of the Zn(II) ion is due to a cation-mediated imine−enamine tautomerization reaction, a new detection method not previously observed for this important cation of clinical concern.

Acknowledgment. The authors thank NSF-EPSCOR (EPS-0554609) and the South Dakota Governor's 2010 Initiative for the purchase of a Bruker SMART APEX II CCD diffractometer. The elemental analyzer was provided by funding from NSF-URC (CHE-0532242). P.N.B. also thanks NSF-EPSCoR (EPS-0903804).

Supporting Information Available. Experimental procedures, crystallographic data, and full spectroscopic data for all new compounds. This material is available free of charge via the Internet at http://pubs.acs.org.

The authors declare no competing financial interest.